A Selenourea-Thiourea Brønsted Acid Catalyst Facilitates Asymmetric Conjugate Additions of Amines to α,β-Unsaturated Esters

Yingfu Lin,[†,‡] William J. Hirschi,[§] Anuj Kunadia,[‡] Anirudra Paul,[†,‡] Ion Ghiviriga,[∥] Khalil A. Abboud,[¶] Rachael W. Karugu,[§] Mathew J. Vetticatt,[*,§] Jennifer S. Hirschi,[*,§] and Daniel Seidel[*,†,‡]

[†]Center for Heterocyclic Compounds, Department of Chemistry, University of Florida, Gainesville, Florida 32611, United States

[‡]Department of Chemistry and Chemical Biology, Rutgers, The State University of New Jersey, Piscataway, New Jersey 08854, United States

[§]Department of Chemistry, Binghamton University, Binghamton, New York 13902, United States

[∥]Center for NMR Spectroscopy, Department of Chemistry, University of Florida, Gainesville, Florida 32611, United States

[¶]Center for X-ray Crystallography, Department of Chemistry, University of Florida, Gainesville, Florida 32611, United States

Supporting Information Placeholder

ABSTRACT: β–Amino esters are obtained with high levels of enantioselectivity via the conjugate addition of cyclic amines to unactivated α,β-unsaturated esters. A related strategy enables the kinetic resolution of racemic cyclic 2-arylamines, using benzyl acrylate as the resolving agent. Reactions are facilitated by an unprecedented selenourea-thiourea organocatalyst. As elucidated by DFT calculations and ^{13}C kinetic isotope effects studies, the rate-limiting and enantiodetermining step of the reaction is the protonation of a zwitterionic intermediate by the catalyst. This represents a rare case in which a thiourea compound functions as an asymmetric Brønsted acid catalyst.

The prevalence of β-amino acids in nature and the utility of this structural motif in drug discovery have inspired the development of numerous synthetic methods.[1] Particularly desirable are approaches that facilitate access to β-amino acid derivatives in catalytic enantioselective fashion.[1] An attractive way in which this can be accomplished is via the well-known conjugate addition of amines to α,β-unsaturated carboxylic acid derivatives.[2] Indeed, a range of methods have been reported that facilitate catalytic enantioselective additions of nitrogen-centered nucleophiles to conjugate acceptors (Figure 1).[3,4] Examples of such reactions include chiral Lewis acid catalyzed conjugate additions of *O*-alkylhydroxylamine to α,β-unsaturated acylpyrazoles, acylpyrroles, and ketones,[5] hydrazoic acid to α,β-unsaturated imides,[6] and amines to α,β-unsaturated nitriles,[7] α,β-unsaturated imides,[8] and maleimides.[9] Asymmetric organocatalytic variants include the addition of TMS azide to α,β-unsaturated imides,[10] *N*-silyloxycarbamates[11] and *N*-heterocycles[12] to α,β-unsaturated aldehydes, *O*-benzylhydroxylamine to α,β-unsaturated acylpyrazoles[13] and α,β-unsaturated acids,[14] amines to nitroalkenes,[15] benzyloxycarbamates to 4,4,4-trifluorocrotonates,[16] indolines to α,β-unsaturated ketones,[17] and hydroxamic acids to quinone imine ketals.[18,19] Intramolecular versions are also known, albeit not with basic amine nucleophiles.[20] Organocatalytic enantioselective additions to unactivated α,β-unsaturated esters are rare with any nucleophile,[21] likely a consequence of their low electrophilicity.[22] There appears to be only a single example of a catalytic enantioselective addition of a challenging basic amine to an α,β-unsaturated ester.[23] Specifically, a polymeric Lewis acidic aluminum complex was reported to catalyze the addition of benzylamine to ethylcinnamate, with the corresponding product being obtained in 82% ee.[23] Here we report the first examples of catalytic enantioselective conjugate additions of basic, cyclic amines to unactivated α,β-unsaturated esters.

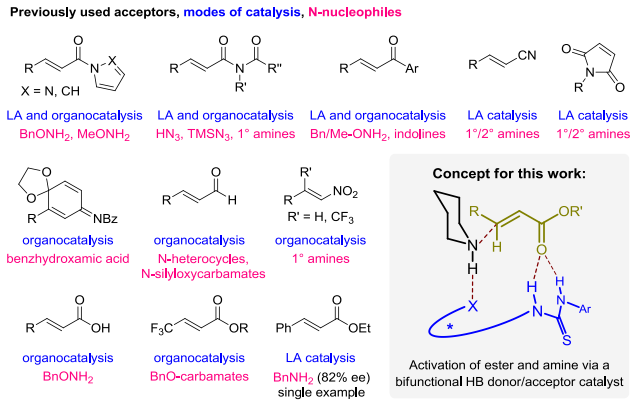

Figure 1. Examples of catalytic enantioselective additions of *N*-nucleophiles to conjugate acceptors, and concept for bifunctional catalysis with α,β-unsaturated ester substrates.

Table 1. Optimization of the Reaction Conditions

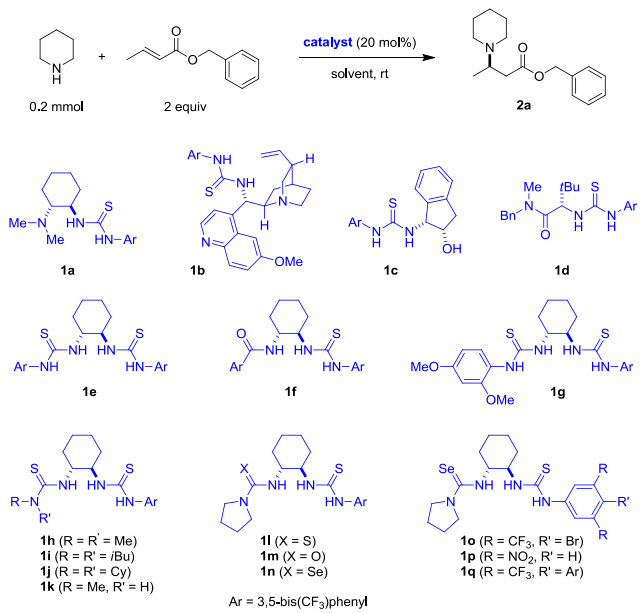

entry	catalyst	solvent (M)	time [h]	yield (%)	ee (%)
1	-	PhMe (2)	24	50	-
2	**1a**	PhMe (2)	23	86	0
3	**1b**	PhMe (2)	22	94	0
4	**1c**	PhMe (2)	20	87	11
5	**1d**	PhMe (2)	20	90	–28
6	**1e**	PhMe (2)	4	93	43
7	**1f**	PhMe (2)	7	91	34
8	**1g**	PhMe (2)	5	93	46
9	**1h**	PhMe (2)	4	93	58
10	**1i**	PhMe (2)	4	92	55
11	**1j**	PhMe (2)	5	95	50
12	**1k**	PhMe (2)	4	94	58
13	**1l**	PhMe (2)	4	92	59
14	**1m**	PhMe (2)	18	92	53
15	**1n**	PhMe (2)	3	93	71
16[a]	**1o**	PhMe (2)	3	93	76
17	**1o**	PhMe (0.5)	16	91	84
18	**1o**	PhMe (0.2)	20	89	86
19	-	PhMe (0.2)	24	trace	-
20	**1o**	TBME (0.2)	24	86	85
21	**1o**	$CHCl_3$ (0.2)	24	92	75
22[a]	**1o**	$PhCF_3$ (0.2)	24	92	79
23	**1o**	PhH (0.2)	24	92	84
24	**1p**	PhMe (0.2)	22	92	85
25	**1q**	PhMe (0.2)	24	92	88
26[b]	**1q**	PhMe (0.2)	34	89	88
27[b,c]	**1q**	PhMe (0.2)	72	90	93

[a] Reaction mixture was partially heterogeneous. [b] Reaction was performed with 10 mol% catalyst. [c] Reaction was performed at –10 °C.

We reasoned that the challenging substrate combination of an unactivated α,β-unsaturated ester and a basic amine nucleophile might be successfully realized through bifunctional organocatalysis (Figure 1).[24] Specifically, an organocatalyst featuring an electron-deficient thiourea functionality was envisioned to activate the α,β-unsaturated ester substrate via hydrogen bonding (HB) to the carbonyl oxygen. Such interactions have been observed in X-ray crystal structures,[25] and are implicated in prior work.[21] A Brønsted basic/HB acceptor site on the catalyst could serve to simultaneously activate the amine nucleophile. The absolute stereochemistry of the resulting product would thus be controlled by a network of HB interactions.

This concept was evaluated with piperidine and benzyl crotonate as summarized in Table 1. Relatively high substrate concentrations in toluene solvent (2 M in piperidine) were initially employed. Under these conditions, in the absence of any catalyst at room temperature, approximately 50% conversion of piperidine was noted after 24 h (entry 1). Well-known bifunctional catalysts **1a**,[26] **1b**,[27] **1c**,[28] and **1d**[29] all modestly accelerated the reaction, albeit with low or no enantioinduction (entries 2–5). Significant rate acceleration was observed with the Nagasawa bisthiourea catalyst **1e**.[30] Encouragingly, product **2a** was obtained with 43% ee (entry 6). Amide-thiourea **1f** provided inferior results (entry 7),[31] suggesting an important role for the second thiourea functionality and prompting the evaluation of several catalysts containing an electron-rich thiourea moiety in addition to an electron-poor one (entries 8–13).[32] Catalysts **1g–l** all outperformed **1e**, with **1l** providing the best results (entry 13). The analogous urea-thiourea **1m** was found to be significantly less reactive and provided **2a** in lower ee (entry 14). However, the corresponding selenourea-thiourea **1n** achieved significantly improved ee while providing further rate acceleration (entry 15). Catalyst **1o** containing an additional bromine substituent to further increase the electron-withdrawing character of the aryl substituent proved better still, despite of not being fully soluble (entry 16). A reduction in piperidine concentration proved beneficial in regard to product ee with 0.2 M being optimal (entry 18). Under these conditions, there was no detectable background reactivity within 24 h (entry 19). Further evaluation of reaction parameters and additional catalysts resulted in the identification of catalyst **1q**, which, at a 10 mol% loading at –10 °C, provided product **2a** in 90% yield and 93% ee (entry 27).

The scope of the reaction is summarized in Scheme 1. A range of cyclic amines participated in the title reaction to provide products **2** with good to excellent levels of enantioselectivity. *P*-methoxybenzylamine, a representative primary amine, provided products with slightly reduced ees. Surprisingly, a significant drop in reactivity was noted with benzyl 2-pentenoate, an observation that could be partially rationalized by our computational model (*vide infra*).[33] Acyclic secondary amines such as diethylamine and *N*-benzylmethylamine provided poor conversions, even in reactions conducted at rt for a period of several days (not shown). α-Branched primary amines such as benzhydrylamine failed to undergo conjugate additions even at a temperature of 40 °C (not shown).

We recently reported a simple one-step method to access cyclic 2-arylamines in racemic form,[34] and wondered whether such substrates could be resolved via a conjugate addition strategy. With few exceptions,[35] small-molecule based catalytic strategies for the kinetic resolution of basic amine substrates typically rely on acylation and are limited to primary amines.[36] There are few solutions to the kinetic resolution of cyclic amines,[37] and no general strategies exist to resolve cyclic 2-arylamines. Following an extensive screen of readily available conjugate acceptors, using 2-phenylpiperidine as the model substrate,[38] commercial benzyl acrylate was identified as a suitable resolving agent. As summarized in Scheme 2, catalyst **1q** facilitated the kinetic resolution of a

number of 2-arylpiperidines and related substrates with good to excellent selectivities.[39] In situ Boc-protection of the unreacted starting material was performed to facilitate product isolation and s-factor analysis.

Scheme 1. Substrate Scope

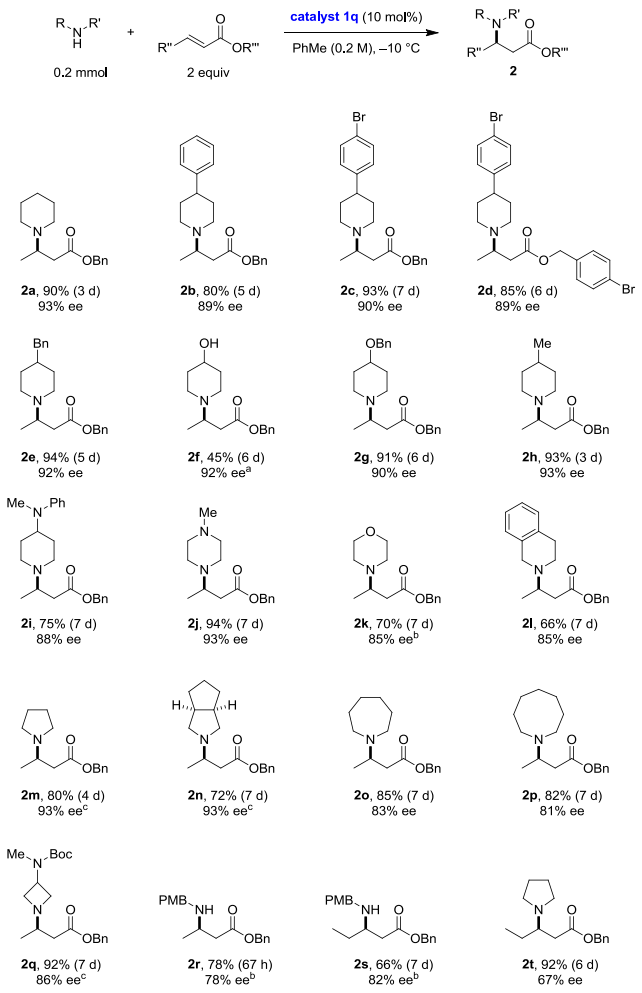

[a] Reaction mixture was partially heterogeneous. [b] Reaction was performed at room temperature. [c] Reaction was performed at a 0.025 M concentration of amine.

Scheme 2. Kinetic Resolution of Cyclic 2-Arylamines.

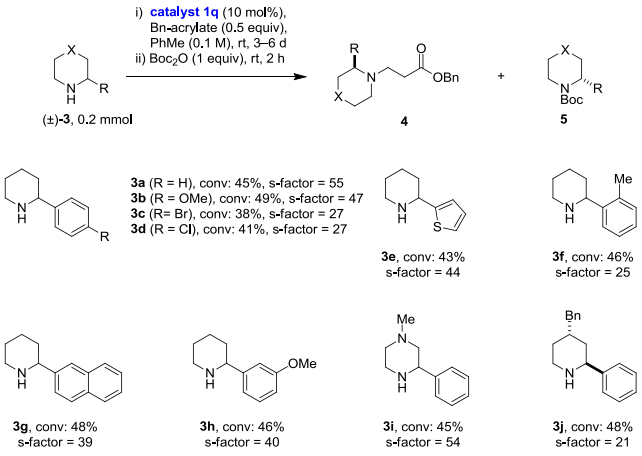

Our next efforts were directed towards understanding the mechanism and origin of enantioselectivity of this novel bifunctional selenourea-thiourea organocatalyzed reaction. The proposed catalytic cycle for the addition of secondary amines to α,β-unsaturated esters involves: [1] initial activation of the ester through H-bonding to the selenourea-thiourea catalyst; [2] conjugate addition of the amine to the activated complex, in the key C–N bond-forming (stereogenic-center-forming) step; and either [3a] direct C-protonation of the zwitterionic enolate intermediate ($\mathbf{2a}_{zwit}$) to form the N-protonated β-amino ester ($\mathbf{2a}_{prot}$), which is subsequently deprotonated to deliver product **2a** and regenerate catalyst **1q** (red pathway, Figure 2), or [3b] the zwitterionic enolate intermediate ($\mathbf{2a}_{zwit}$) undergoes an intramolecular proton transfer to form $\mathbf{2a}_{enol}$ followed by tautomerization to give **2a** and regenerate **1q** (blue pathway, Figure 2).

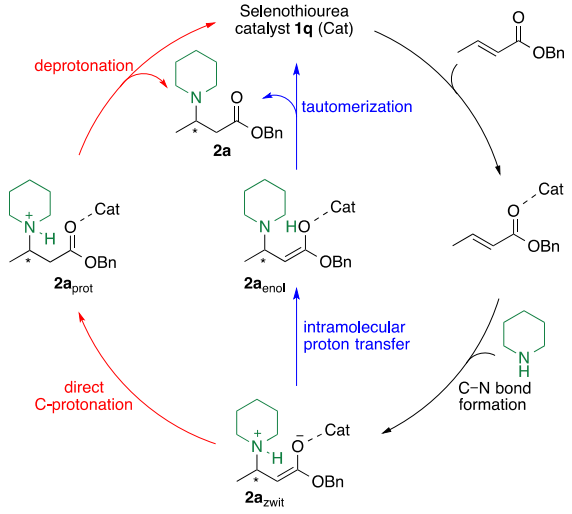

Figure 2. Proposed catalytic cycle for the addition of amines to α,β-unsaturated esters catalyzed by a selenourea-thiourea catalyst. The stereogenic center is formed during C–N bond formation. Subsequent proton transfers may follow an intramolecular proton transfer path (shown in blue) or direct C-protonation (shown in red).

In order to understand the origin of enantioselectivity, we decided to model the stereogenic-center-forming step in the reaction of piperidine and benzyl crotonate catalyzed by **1q** using density functional theory (DFT) calculations. Transition structures (TS) for the C–N bond-forming step leading to formation of the *R*- and *S*- enantiomers of the β-amino ester ($\mathbf{2a}_{zwit}$) were computed using the B3LYP method[40] with a split 6-31G* (C,H,O,N,F)/6-31+G** (S, Se) basis set as implemented in Gaussian '09.[41] Single-point energy calculations were performed using B3LYP-D3(BJ)[42]/6-311++G** with a PCM solvent model[43] for toluene. Relative energies presented herein are the extrapolated Gibbs free energy obtained by adding the free energy correction to the high-level single point energy computed for each structure. The free energies were corrected using Grimme's quasi rigid rotor - harmonic oscillator (qRRHO) approach, which raises vibrational frequencies that are below 100 cm^{-1} to 100 cm^{-1}.[44] This approach is routinely utilized to evaluate reactivity and selectivity in similar catalytic systems.[45]

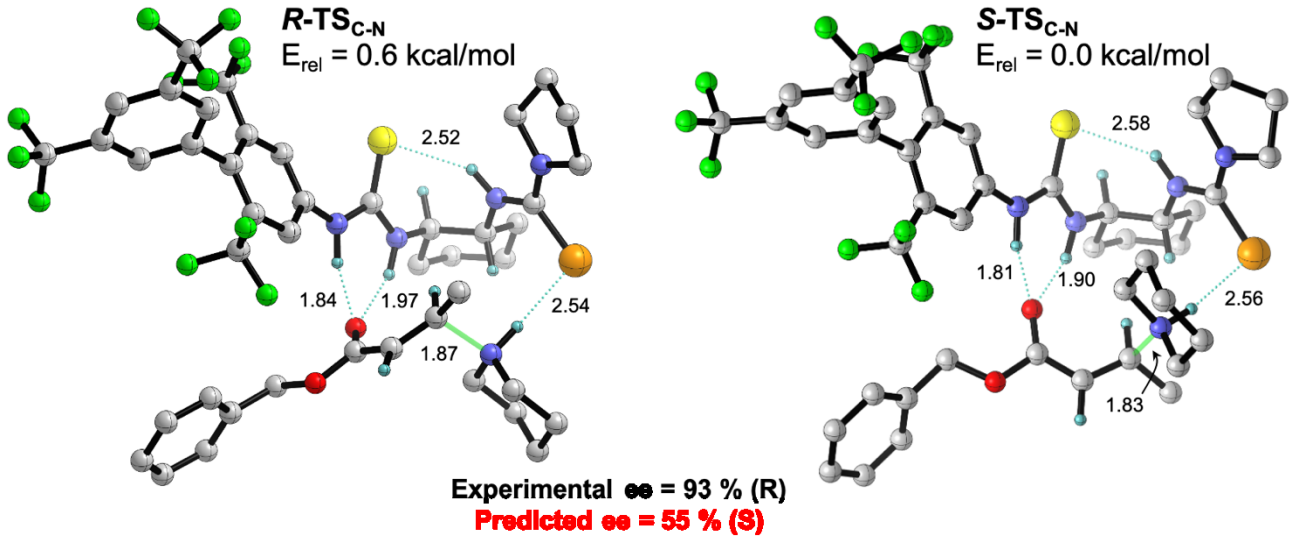

Figure 3. Lowest energy transition structures for C–N bond-formation leading to (*R*)- and (*S*)-enantiomers of $\mathbf{2a}_{zwit}$

Following a thorough conformational search conducted via systematic variation of catalyst and reactant geometries,[46] we identified the lowest energy C–N bond-forming transition structures leading to both enantiomers of $\mathbf{2a}_{zwit}$ - ***R*-TS$_{C-N}$** and ***S*-TS$_{C-N}$** (Figure 3). Both TSs involve β-attack of piperidine on the *s*-cis conformation of benzyl crotonate, which is more favored than the corresponding *s*-trans conformation.[47] In both of these TSs, the thiourea NHs activate the ester carbonyl by dual H-bonding (1.84 Å /1.97 Å ***R*-TS$_{C-N}$** and 1.81 Å /1.90 Å ***S*-TS$_{C-N}$**) while the selenourea directs the attack of piperidine via an H-bonding interaction between the selenium and the amine proton of piperidine (2.54 Å ***R*-TS$_{C-N}$** and 2.56 Å ***S*-TS$_{C-N}$**). This catalyst conformation is the most favored since it is stabilized by an intramolecular H-bonding interaction between the two arms of the catalyst, i.e. between the thiourea sulfur and the NH of the selenourea moiety. A careful analysis of ***R*-TS$_{C-N}$** and ***S*-TS$_{C-N}$** reveals that the key C–N bond-forming distances (1.87 Å ***R*-TS$_{C-N}$** and 1.83 Å ***S*-TS$_{C-N}$**) and all H-bonding interactions primarily responsible for transition state stabilization (*vide supra*) are almost identical for both TSs. Slightly stronger dual H-bonding interactions in ***S*-TS$_{C-N}$** make it lower in energy than ***R*-TS$_{C-N}$** resulting in a predicted ee of 55% (*S*) at -10 °C. This is inconsistent with the experimental ee of 93% (*R*).

Since the extensive transition state search for C–N bond formation structures results in an incorrect prediction of enantioselectivity, we contemplated that the rate- and enantio-determining step occurs after the stereogenic-center-forming step. To test this hypothesis, we measured ^{13}C kinetic isotope effects (KIEs) for benzyl crotonate using Singleton's ^{13}C NMR methodology for starting materials at natural abundance.[48] Two independent reactions of benzyl crotonate and piperidine were taken to 75±2 % and 79±2 % conversion with respect to the ester. Unreacted benzyl crotonate was reisolated and the ^{13}C isotopic composition was compared to samples of benzyl crotonate not subjected to reaction conditions. From the changes in relative isotopic composition and the fractional conversion, ^{13}C KIEs were determined in a standard way.[38]

Key results are the unity KIE observed at the β-carbon and the normal KIE of ~1.5% on the α-carbon (Figure 4). If C–N bond-formation is the first irreversible step in the catalytic cycle for benzyl crotonate, a normal KIE on the β-carbon is expected; however, the observed unity KIE is qualitatively consistent with reversible C–N bond-formation. Secondly, an observed normal KIE of ~1.5% on the α-carbon suggests that α-protonation is likely the first irreversible step in the catalytic cycle. The results qualitatively validate our hypothesis that the C–N bond-forming step is reversible and the rate- and enantio-determining step occurs *after* this stereogenic-center-forming step – a finding that has important consequences for our future efforts in expanding the scope of this reaction.

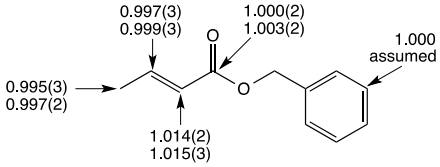

Figure 4. Experimental ^{13}C KIEs for benzyl crotonate (numbers in parenthesis represent the standard deviation in the last digit as determined from six independent measurements)

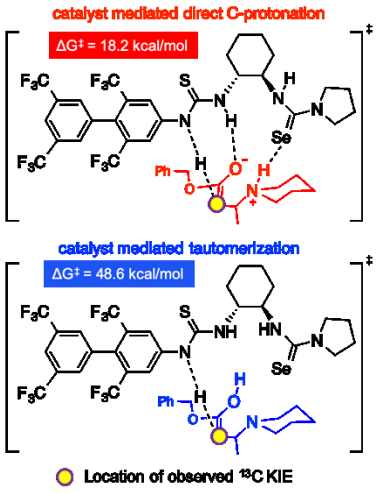

Figure 5. Possible transition states consistent with experimental KIEs

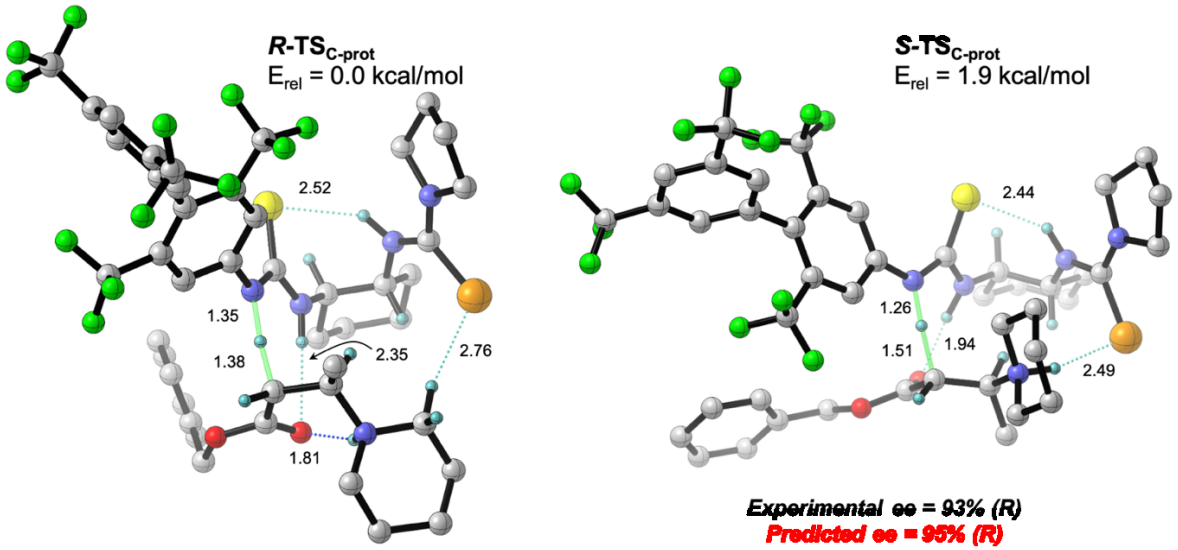

Figure 6. Lowest energy transition structures for catalyst mediated direct C-protonation of (*R*)- and (*S*)-enantiomers of **2a**$_{zwit}$

Experimental ^{13}C KIEs suggest the origin of enantioselectivity is best understood by analysis of the enantiomeric transition states for the α-carbon protonation step. In the absence of a more acidic proton on the catalyst or an external Brønsted acid in the system, we considered that one of the thiourea NHs is most likely involved in the α-protonation event (Figure 5). Based on this assumption, two possibilities emerge that are qualitatively consistent with a normal ^{13}C KIE on the α-carbon – catalyst mediated tautomerization (Figure 5, bottom panel) or catalyst mediated direct C-protonation (Figure 5, top panel).[49]

Accordingly, we investigated both pathways for α-protonation using DFT calculations (*vide supra*). While intramolecular proton transfer from N to O of **2a**$_{zwit}$ to **2a**$_{enol}$ is facile (not shown, $\Delta G^{\ddagger}$ = 18.1 kcal/mol for proton transfer from *R*-**2a**$_{zwit}$), the ensuing catalyst mediated tautomerization of **2a**$_{enol}$ to **2a** is prohibitively high in energy (Figure 5, $\Delta G^{\ddagger}$ = 48.7 kcal/mol).[45] On the other hand, the catalyst mediated C-protonation is energetically accessible (Figure 5, $\Delta G^{\ddagger}$ = 18.2 kcal/mol). Inaccessibility of the intramolecular proton transfer/tautomerization pathway led us to turn our explorations to the catalyst-mediated C-protonation as the rate- and enantio-selectivity determining step. Involvement of the thiourea catalyst directly as a Brønsted acid in the mechanism has only been reported in two instances in the literature,[50] thus representing a new mode of catalysis, which should be considered in the development of future systems.[51]

In the lowest energy transition structure for direct protonation of *R*-**2a**$_{zwit}$ (Figure 6, ***R*-TS$_{C\text{-}prot}$**), the enolate adopts a geometry with strong intramolecular H-bonding interactions between the protonated piperidine and the enolate oxygen (1.81 Å). One of the thiourea NHs is loosely bound to the enolate oxygen (2.35 Å) while the other (more acidic) thiourea NH is transferred to the α-carbon of the ester. Selenium is engaged in a weak non-conventional CH···Se interaction with one of the α-CHs of the piperidine moiety (2.76 Å). A significantly altered arrangement is observed for the lowest energy transition structure for direct protonation of *S*-**2a**$_{zwit}$ (Figure 6, ***S*-TS$_{C\text{-}prot}$**). The enolate oxygen is bound via a strong H-bonding interaction with one of the thiourea NHs (1.94 Å) during the protonation event. Protonated piperidine NH is engaged in an H-bonding interaction with selenium (2.49 Å) (unlike ***R*-TS$_{C\text{-}prot}$**, where the same NH is engaged in a stronger intramolecular H-bond with the enolate oxygen). Another key difference between the two TSs is the extent of proton transfer from the thiourea NH to the α-carbon of the enolate (1.35 Å and 1.26 Å for the breaking thiourea N-H bond in ***R*-TS$_{C\text{-}prot}$** and ***S*-TS$_{C\text{-}prot}$**, respectively). These differences in stabilizing interactions at the enantiomeric transition states for catalyst-mediated direct α-C-protonation result in ***R*-TS$_{C\text{-}prot}$** being 1.9 kcal/mol lower in free energy than ***S*-TS$_{C\text{-}prot}$**; this corresponds to a predicted 95% ee (*R*) at -10 °C, which is in excellent agreement with the 93% ee (*R*) observed experimentally. Additional support for direct α-C-protonation as the rate- and enantioselectivity determining step was obtained by modeling the two transition structures by replacing the selenium atom with sulfur. With this sulfur analogue of catalyst **1q**, we predicted a 59% ee which is in good agreement with the experimental ee of 62%.[38] Finally, we also probed the effect of varying the β-substituent of the ester from methyl to ethyl by modeling the ***R*-TS$_{C\text{-}prot}$** and ***S*-TS$_{C\text{-}prot}$** for the β-ethyl substituted benzyl ester. These analogous transition structures gave a drop in the predicted ee to 80%, which is a slight over-estimation (0.7 kcal/mol) of the experimental ee of 47%. However, these calculations qualitatively predict the drop in ee experimentally observed with the bulkier β-ethyl substituent.[38]

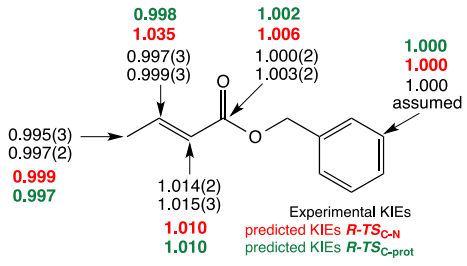

Figure 7. Comparison of experimental and predicted KIEs for the C–N bond-forming transition structure ***R*-TS$_{C\text{–}N}$** (shown in red) and the direct C-protonation transition structure ***R*-TS$_{C\text{-}prot}$** (shown in green)

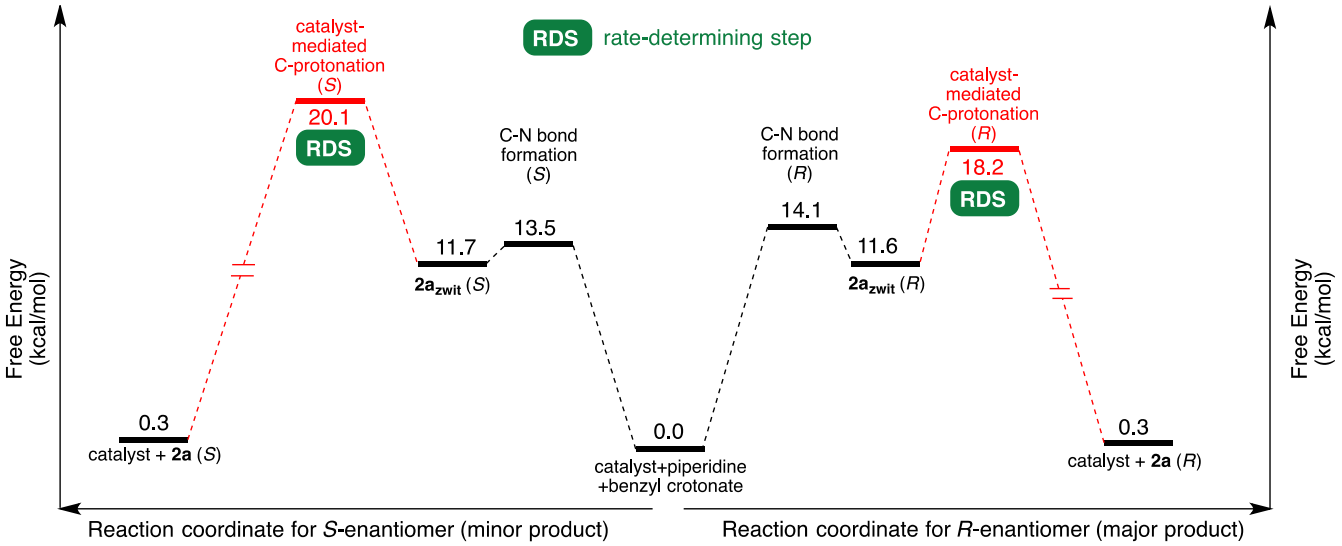

Figure 8. Computed reaction coordinate diagram (qRRHO) depicting the proposed pathway leading to (*R*)- and (*S*)-enantiomers of **2a**

As a key step in the quantitative interpretation of our experimental KIEs, we predict ^{13}C KIEs from the scaled vibrational frequencies using the program ISOEFF98 for both ***R*-TS$_{C-N}$** and ***R*-TS$_{C\text{-}prot}$**, then applying a Wigner tunneling correction to all predicted KIEs.[52–54] The large ^{13}C KIE of 1.035 predicted for the β-carbon in ***R*-TS$_{C-N}$** (Figure 7, red numbers) quantitatively eliminates C–N bond-formation as the rate-determining step. On the other hand, the predicted KIEs for ***R*-TS$_{C\text{-}prot}$** (Figure 7, green numbers) are in excellent agreement with experimental KIEs for all carbons, lending further support for rate-determining catalyst mediated direct α-C-protonation.

Finally, the computed reaction coordinate diagram summarizes the relevant energies from our theoretical investigation (Figure 8). Energies of all TSs and intermediates are computed relative to the free energy of separated catalyst and starting materials (Figure 8, catalyst + piperidine + benzyl crotonate). To the left of the starting materials is the reaction pathway leading to (*S*)-**2a** (minor product) and to the right is the corresponding pathway leading to (*R*)-**2a** (major product). As discussed earlier, the C–N bond forming step is reversible and the enantioselectivity is determined at the rate-determining direct *C*-protonation step.[55]

In summary, we have achieved highly enantioselective conjugate additions of cyclic amines to unactivated α,β-unsaturated esters. This strategy is applicable to the kinetic resolution of cyclic 2-arylamines. A novel bifunctional selenourea-thiourea was identified in the course of this study. Experimental and predicted KIEs, free energy estimates, and enantioselectivity predictions all lend strong support to a reaction mechanism that proceeds via reversible C–N bond-formation to form a β-amino enolate. This is followed by rate- and enantioselectivity determining protonation by one of the thiourea NHs, which functions as a Brønsted acid. The transition structure, in which a thiourea compound functions as an asymmetric Brønsted acid, should serve as a guide for further development of this new mode of catalysis by chiral thiourea organocatalysts.

ASSOCIATED CONTENT

Supporting Information

Experimental procedures and characterization data, including X-ray crystal structures of catalyst **1q** and product **2d**. Kinetic isotope effects studies. Details of the theoretical studies along with coordinates and energies of all calculated structures. This material is available free of charge via the Internet at http://pubs.acs.org.

AUTHOR INFORMATION

Corresponding Authors

* jhirschi@binghamton.edu
* vetticatt@binghamton.edu
* seidel@chem.ufl.edu

Notes

The authors declare no competing financial interests.

ACKNOWLEDGMENT

This material is based upon work supported by the National Science Foundation under CHE–1806747 and CHE–1856613 (grants to D.S.). M.J.V. and J.S.H acknowledge support from NIGMS - R01 GM126283 and the XSEDE Science Gateways Program, which is supported by National Science Foundation grant number ACI-1548562. We further acknowledge the National Science Foundation (grant# 1828064 to K.A.A.) and the University of Florida for funding the purchase of the X-ray equipment.

REFERENCES

(1) Selected reviews on β-amino acids: a) Asymmetric synthesis of ß-amino acids and α-substituted β-amino acids. Cardillo, G.; Tomasini, C. *Chem. Soc. Rev.* **1996**, *25*, 117-128; b) Recent advances in the stereoselective synthesis of β-amino acids. Liu, M.; Sibi, M. P. *Tetrahedron* **2002**, *58*, 7991-8035; c) Enantioselective Preparation of β²-Amino Acid Derivatives for β-Peptide Synthesis. Seebach, D.; Beck, A. K.; Capone, S.; Deniau, G.; Grošelj, U.; Zass, E. *Synthesis* **2009**, *2009*, 1-32; d) Recent advances in the catalytic asymmetric synthesis of beta-amino acids. Weiner, B.; Szymanski, W.; Janssen, D. B.; Minnaard, A. J.; Feringa, B. L. *Chem. Soc. Rev.* **2010**, *39*, 1656-1691.

(2) Aza-Michael reaction: achievements and prospects. Alexander Yu, R. *Russ. Chem. Rev.* **2011**, *80*, 197.

(3) Selected reviews on asymmetric conjugate additions with N-nucleophiles: a) A Catalytic Enantioselective Aza-Michael Reaction: Novel Protocols for Asymmetric Synthesis of β-Amino Carbonyl Compounds. Xu, L.-W.; Xia, C.-G. *Eur. J. Org. Chem.* **2005**, *2005*, 633-639; b) The asymmetric aza-Michael reaction. A review. Vicario, J. L.; Badía, D.; Carrillo, L.; Etxebarria, J.; Reyes, E.; Ruiz, N. *Org. Prep. Proced. Int.* **2005**, *37*, 513-538; c) Organocatalytic Asymmetric Aza-Michael Additions. Enders, D.; Wang, C.; Liebich, J. X. *Chem. Eur. J.* **2009**, *15*, 11058-11076; d) Recent advances and applications in asymmetric aza-Michael addition chemistry. Krishna, P. R.; Sreeshailam, A.; Srinivas, R. *Tetrahedron* **2009**, *65*, 9657-9672; e) Advances and Applications in Organocatalytic Asymmetric aza-Michael Addition. Wang, J.; Li, P.; Choy, P. Y.; Chan, A. S. C.; Kwong, F. Y. *ChemCatChem* **2012**, *4*, 917-925; f) Recent advances in the asymmetric synthesis of pharmacology-relevant nitrogen heterocycles via stereoselective aza-Michael reactions. Vinogradov, M. G.; Turova, O. V.; Zlotin, S. G. *Org. Biomol. Chem.* **2019**, *17*, 3670-3708.

(4) Cutting-Edge and Time-Honored Strategies for Stereoselective Construction of C–N Bonds in Total Synthesis. Mailyan, A. K.; Eickhoff, J. A.; Minakova, A. S.; Gu, Z.; Lu, P.; Zakarian, A. *Chem. Rev.* **2016**, *116*, 4441-4557.

(5) a) Chiral Lewis Acid Catalysis in Conjugate Additions of O-Benzylhydroxylamine to Unsaturated Amides. Enantioselective Synthesis of β-Amino Acid Precursors. Sibi, M. P.; Shay, J. J.; Liu, M.; Jasperse, C. P. *J. Am. Chem. Soc.* **1998**, *120*, 6615-6616; b) Catalytic conversion of conjugated enones into optically active α-keto aziridines using chiral rare earth metal complexes. Sugihara, H.; Daikai, K.; Jin, X. L.; Furuno, H.; Inanaga, J. *Tetrahedron Lett.* **2002**, *43*, 2735-2739; c) Chiral rare earth metal complex-catalyzed conjugate addition of O-alkylhydroxylamines. An efficient synthetic entry into optically active 2-acyl aziridines. Jin, X. L.; Sugihara, H.; Daikai, K.; Tateishi, H.; Jin, Y. Z.; Furuno, H.; Inanaga, J. *Tetrahedron* **2002**, *58*, 8321-8329; d) Heterobimetallic Catalysis in Asymmetric 1,4-Addition of O-Alkylhydroxylamine to Enones. Yamagiwa, N.; Matsunaga, S.; Shibasaki, M. *J. Am. Chem. Soc.* **2003**, *125*, 16178-16179; e) Lewis Acid–Lewis Acid Heterobimetallic Cooperative Catalysis: Mechanistic Studies and Application in Enantioselective Aza-Michael Reaction. Yamagiwa, N.; Qin, H.; Matsunaga, S.; Shibasaki, M. *J. Am. Chem. Soc.* **2005**, *127*, 13419-13427.

(6) Asymmetric Synthesis of β-Amino Acid Derivatives via Catalytic Conjugate Addition of Hydrazoic Acid to Unsaturated Imides. Myers, J. K.; Jacobsen, E. N. *J. Am. Chem. Soc.* **1999**, *121*, 8959-8960.

(7) Ni(II) Complexes containing chiral tridentate phosphines as new catalysts for the hydroamination of activated olefins. Fadini, L.; Togni, A. *Chem. Commun.* **2003**, 30-31.

(8) Amine-Salt-Controlled, Catalytic Asymmetric Conjugate Addition of Various Amines and Asymmetric Protonation. Hamashima, Y.; Somei, H.; Shimura, Y.; Tamura, T.; Sodeoka, M. *Org. Lett.* **2004**, *6*, 1861-1864.

(9) Calcium(II)-catalyzed enantioselective conjugate additions of amines. Uno, B. E.; Dicken, R. D.; Redfern, L. R.; Stern, Charlotte M.; Krzywicki, G. G.; Scheidt, K. A. *Chem. Sci.* **2018**, *9*, 1634-1639.

(10) a) Asymmetric Conjugate Addition of Azide to α,β-Unsaturated Carbonyl Compounds Catalyzed by Simple Peptides. Horstmann, T. E.; Guerin, D. J.; Miller, S. J. *Angew. Chem. Int. Ed.* **2000**, *39*, 3635-3638; b) Asymmetric Azidation–Cycloaddition with Open-Chain Peptide-Based Catalysts. A Sequential Enantioselective Route to Triazoles. Guerin, D. J.; Miller, S. J. *J. Am. Chem. Soc.* **2002**, *124*, 2134-2136.

(11) Enantioselective Organocatalytic Amine Conjugate Addition. Chen, Y. K.; Yoshida, M.; MacMillan, D. W. C. *J. Am. Chem. Soc.* **2006**, *128*, 9328–9329.

(12) Enantioselective Organocatalytic Conjugate Addition of N Heterocycles to α,β-Unsaturated Aldehydes. Dinér, P.; Nielsen, M.; Marigo, M.; Jørgensen, K. A. *Angew. Chem. Int. Ed.* **2007**, *46*, 1983-1987.

(13) Organocatalysis in Conjugate Amine Additions. Synthesis of b-Amino Acid Derivatives. Sibi, M. P.; Itoh, K. *J. Am. Chem. Soc.* **2007**, *129*, 8064–8065.

(14) a) Mechanistic Insight into Asymmetric Hetero-Michael Addition of α,β-Unsaturated Carboxylic Acids Catalyzed by Multifunctional Thioureas. Hayama, N.; Kuramoto, R.; Földes, T.; Nishibayashi, K.; Kobayashi, Y.; Pápai, I.; Takemoto, Y. *J. Am. Chem. Soc.* **2018**, *140*, 12216-12225; b) Catalytic asymmetric aza-Michael addition of fumaric monoacids with multifunctional thiourea/boronic acids. Michigami, K.; Murakami, H.; Nakamura, T.; Hayama, N.; Takemoto, Y. *Org. Biomol. Chem.* **2019**, *17*, 2331-2335.

(15) a) Chiral Arylaminophosphonium Barfates as a New Class of Charged Brønsted Acid for the Enantioselective Activation of Nonionic Lewis Bases. Uraguchi, D.; Nakashima, D.; Ooi, T. *J. Am. Chem. Soc.* **2009**, *131*, 7242-7243; b) Highly Enantioselective Aza-Michael Reaction between Alkyl Amines and β-Trifluoromethyl β-Aryl Nitroolefins. Wang, L.; Chen, J.; Huang, Y. *Angew. Chem. Int. Ed.* **2015**, *54*, 15414-15418.

(16) Asymmetric addition of a nitrogen nucleophile to an enoate in the presence of a chiral phase-transfer catalyst: A novel approach toward enantiomerically enriched protected β-amino acids. Weiß, M.; Borchert, S.; Rémond, E.; Jugé, S.; Gröger, H. *Heteroatom Chem.* **2012**, *23*, 202-209.

(17) Bifunctional cinchona alkaloid-squaramide-catalyzed highly enantioselective aza-Michael addition of indolines to α,β-unsaturated ketones. Ghosh, A. K.; Zhou, B. *Tetrahedron Lett.* **2013**, *54*, 3500-3502.

(18) Boronic Acid-Catalyzed, Highly Enantioselective Aza-Michael Additions of Hydroxamic Acid to Quinone Imine Ketals. Hashimoto, T.; Gálvez, A. O.; Maruoka, K. *J. Am. Chem. Soc.* **2015**, *137*, 16016-16019.

(19) For an enantioselective radical-based approach to β-amination, see: Enantioselective catalytic β-amination through proton-coupled electron transfer followed by stereocontrolled radical–radical coupling. Zhou, Z.; Li, Y.; Han, B.; Gong, L.; Meggers, E. *Chem. Sci.* **2017**, *8*, 5757-5763.

(20) a) A general overview of the organocatalytic intramolecular aza-Michael reaction. Sánchez-Roselló, M.; Aceña, J. L.; Simón-Fuentes, A.; del Pozo, C. *Chem. Soc. Rev.* **2014**, *43*, 7430-7453. Recent examples: b) Cinchonamine Squaramide Catalyzed Asymmetric aza-Michael Reaction: Dihydroisoquinolines and Tetrahydropyridines. Roy, T. K.; Parhi, B.; Ghorai, P. *Angew. Chem. Int. Ed.* **2018**, *57*, 9397-9401; c) Combining traditional 2D and modern physical organic-derived descriptors to predict enhanced enantioselectivity for the key aza-Michael conjugate addition in the synthesis of Prevymis™ (letermovir). Metsänen, T. T.; Lexa, K. W.; Santiago, C. B.; Chung, C. K.; Xu, Y.; Liu, Z.; Humphrey, G. R.; Ruck, R. T.; Sherer, E. C.; Sigman, M. S. *Chem. Sci.* **2018**, *9*, 6922-6927.

(21) See: Enantioselective bifunctional iminophosphorane catalyzed sulfa-Michael addition of alkyl thiols to unactivated β-substituted-α,β-unsaturated esters. Yang, J.; Farley, A. J. M.; Dixon, D. J. *Chem. Sci.* **2017**, *8*, 606-610, and references cited therein.

(22) Quantification and Theoretical Analysis of the Electrophilicities of Michael Acceptors. Allgäuer, D. S.; Jangra, H.; Asahara, H.; Li, Z.; Chen, Q.; Zipse, H.; Ofial, A. R.; Mayr, H. *J. Am. Chem. Soc.* **2017**, *139*, 13318-13329.

(23) A New Polymer-Anchored Chiral Catalyst for Asymmetric Michael Addition Reactions. Sundararajan, G.; Prabagaran, N. *Org. Lett.* **2001**, *3*, 389-392.

(24) Selected reviews: a) Recognition and activation by ureas and thioureas: stereoselective reactions using ureas and thioureas as hydrogen-bonding donors. Takemoto, Y. *Org. Biomol. Chem.* **2005**, *3*, 4299–4306; b) Small-molecule H-bond donors in asymmetric cataly-

sis. Doyle, A. G.; Jacobsen, E. N. *Chem. Rev.* **2007**, *107*, 5713–5743; c) Asymmetric catalysis with bifunctional cinchona alkaloid-based urea and thiourea organocatalysts. Connon, S. J. *Chem. Commun.* **2008**, 2499-2510; d) Asymmetric organocatalytic reactions by bifunctional amine-thioureas. Siau, W.-Y.; Wang, J. *Catal. Sci. Technol.* **2011**, *1*, 1298-1310; e) Bifunctional primary amine-thioureas in asymmetric organocatalysis. Serdyuk, O. V.; Heckel, C. M.; Tsogoeva, S. B. *Org. Biomol. Chem.* **2013**, *11*, 7051-7071; f) Recent advances in asymmetric organocatalysis mediated by bifunctional amine-thioureas bearing multiple hydrogen-bonding donors. Fang, X.; Wang, C.-J. *Chem. Commun.* **2015**, *51*, 1185-1197.

(25) Examples: a) Towards predictable transmembrane transport: QSAR analysis of anion binding and transport. Busschaert, N.; Bradberry, S. J.; Wenzel, M.; Haynes, C. J. E.; Hiscock, J. R.; Kirby, I. L.; Karagiannidis, L. E.; Moore, S. J.; Wells, N. J.; Herniman, J.; Langley, G. J.; Horton, P. N.; Light, M. E.; Marques, I.; Costa, P. J.; Felix, V.; Frey, J. G.; Gale, P. A. *Chem. Sci.* **2013**, *4*, 3036-3045; b) Organophotocatalysis: Insights into the Mechanistic Aspects of Thiourea-Mediated Intermolecular [2+2] Photocycloadditions. Vallavoju, N.; Selvakumar, S.; Pemberton, B. C.; Jockusch, S.; Sibi, M. P.; Sivaguru, J. *Angew. Chem. Int. Ed.* **2016**, 55, 5446-5451.

(26) Enantioselective Michael reaction of malonates to nitroolefins catalyzed by bifunctional organocatalysts. Okino, T.; Hoashi, Y.; Takemoto, Y. *J. Am. Chem. Soc.* **2003**, *125*, 12672–12673.

(27) Highly enantioselective conjugate addition of nitromethane to chalcones using bifunctional cinchona organocatalysts. Vakulya, B.; Varga, S.; Csámpai, A.; Soós, T. *Org. Lett.* **2005**, *7*, 1967–1969.

(28) Catalytic enantioselective Friedel-Crafts alkylation of indoles with nitroalkenes by using a simple thiourea organocatalyst. Herrera, R. P.; Sgarzani, V.; Bernardi, L.; Ricci, A. *Angew. Chem. Int. Ed.* **2005**, *44*, 6576–6579.

(29) Enantioselective Thiourea-Catalyzed Additions to Oxocarbenium Ions. Reisman, S. E.; Doyle, A. G.; Jacobsen, E. N. *J. Am. Chem. Soc.* **2008**, *130*, 7198–7199.

(30) Development of bis-thiourea-type organocatalyst for asymmetric Baylis-Hillman reaction. Sohtome, Y.; Tanatani, A.; Hashimoto, Y.; Nagasawa, K. *Tetrahedron Lett.* **2004**, *45*, 5589–5592.

(31) Merging Nucleophilic and Hydrogen Bonding Catalysis: An Anion Binding Approach to the Kinetic Resolution of Propargylic Amines. Klauber, E. G.; De, C. K.; Shah, T. K.; Seidel, D. *J. Am. Chem. Soc.* **2010**, *132*, 13624-13626.

(32) Direct Formation of Oxocarbenium Ions under Weakly Acidic Conditions: Catalytic Enantioselective Oxa-Pictet–Spengler Reactions. Zhao, C.; Chen, S. B.; Seidel, D. *J. Am. Chem. Soc.* **2016**, *138*, 9053-9056.

(33) Other α,β-unsaturated ester substrates also provided unfavorable results. For instance, addition of piperidine to benzyl cinnamate proved sluggish and provided the corresponding product in only 51% ee (reaction conducted at rt). α,β-Unsaturated esters with α-substituents such as benzyl tiglate were found to be unreactive.

(34) a) Direct α-C–H bond functionalization of unprotected cyclic amines. Chen, W.; Ma, L.; Paul, A.; Seidel, D. *Nat. Chem.* **2018**, *10*, 165; b) α-Functionalization of Cyclic Secondary Amines: Lewis Acid Promoted Addition of Organometallics to Transient Imines. Paul, A.; Seidel, D. *J. Am. Chem. Soc.* **2019**, *141*, 8778-8782.

(35) Asymmetric Catalysis of the Carbonyl-Amine Condensation: Kinetic Resolution of Primary Amines. Das, S.; Majumdar, N.; De, C. K.; Kundu, D. S.; Döhring, A.; Garczynski, A.; List, B. *J. Am. Chem. Soc.* **2017**, *139*, 1357-1359.

(36) Selected examples: a) Kinetic resolution of amines by a nonenzymatic acylation catalyst. Arai, S.; Bellemin-Laponnaz, S.; Fu, G. C. *Angew. Chem. Int. Ed.* **2001**, *40*, 234–236; b) Asymmetric direct amide synthesis by kinetic amine resolution: a chiral bifunctional aminoboronic acid catalyzed reaction between a racemic amine and an achiral carboxylic acid. Arnold, K.; Davies, B.; Herault, D.; Whiting, A. *Angew. Chem., Int. Ed.* **2008**, *47*, 2673-2676; c) A Dual-Catalysis Anion-Binding Approach to the Kinetic Resolution of Amines: Insights into the Mechanism via a Combined Experimental and Computational Study. Mittal, N.; Lippert, K. M.; De, C. K.; Klauber, E. G.; Emge, T. J.; Schreiner, P. R.; Seidel, D. *J. Am. Chem. Soc.* **2015**, *137*, 5748-5758.

(37) a) Catalytic Kinetic Resolution of Cyclic Secondary Amines. Binanzer, M.; Hsieh, S. Y.; Bode, J. W. *J. Am. Chem. Soc.* **2011**, *133*, 19698-19701; b) Concerted Amidation of Activated Esters: Reaction Path and Origins of Selectivity in the Kinetic Resolution of Cyclic Amines via N-Heterocyclic Carbenes and Hydroxamic Acid Cocatalyzed Acyl Transfer. Allen, S. E.; Hsieh, S.-Y.; Gutierrez, O.; Bode, J. W.; Kozlowski, M. C. *J. Am. Chem. Soc.* **2014**, *136*, 11783-11791; c) Catalytic Kinetic Resolution of Disubstituted Piperidines by Enantioselective Acylation: Synthetic Utility and Mechanistic Insights. Wanner, B.; Kreituss, I.; Gutierrez, O.; Kozlowski, M. C.; Bode, J. W. *J. Am. Chem. Soc.* **2015**, *137*, 11491-11497; d) Iron-Catalyzed Aerobic Dehydrogenative Kinetic Resolution of Cyclic Secondary Amines. Lu, R.; Cao, L.; Guan, H.; Liu, L. *J. Am. Chem. Soc.* **2019**, *141*, 6318-6324.

(38) See the Supporting Information for details.

(39) 2-Arylamines with different ring sizes were resolved with lower efficiency. For instance, 2-phenylpyrrolidine and 2-phenylazepane were resolved with s-factors of 9.4 and 5.7, respectively.

(40) Density-functional thermochemistry. III. The role of exact exchange. Becke, A. D. *J. Chem. Phys.* **1993**, *98*, 5648–5652.

(41) Frisch, M. J.; Trucks, G. W.; Schlegel, H. B.; Scuseria, G. E.; Robb, M. A.; Cheeseman, J. R.; Scalmani, G.; Barone, V.; Mennucci, B.; Petersson, G. A.; Nakatsuji, H.; Caricato, M.; Li, X.; Hratchian, H. P.; Izmaylov, A. F.; Bloino, J.; Zheng, G.; Sonnenberg, J. L.; Hada, M.; Ehara, M.; Toyota, K.; Fukuda, R.; Hasegawa, J.; Ishida, M.; Nakajima, T.; Honda, Y.; Kitao, O.; Nakai, H.; Vreven, T.; Montgomery, J. A., Jr.; Peralta, J. E.; Ogliaro, F.; Bearpark, M.; Heyd, J. J.; Brothers, E.; Kudin, K. N.; Staroverov, V. N.; Kobayashi, R.; Normand, J.; Raghavachari, K.; Rendell, A.; Burant, J. C.; Iyengar, S. S.; Tomasi, J.; Cossi, M.; Rega, N.; Millam, J. M.; Klene, M.; Knox, J. E.; Cross, J. B.; Bakken, V.; Adamo, C.; Jaramillo, J.; Gomperts, R.; Stratmann, R. E.; Yazyev, O.; Austin, A. J.; Cammi, R.; Pomelli, C.; Ochterski, J. W.; Martin, R. L.; Morokuma, K.; Zakrzewski, V. G.; Voth, G. A.; Salvador, P.; Dannenberg, J. J.; Dapprich, S.; Daniels, A. D.; Farkas, Ö.; Foresman, J. B.; Ortiz, J. V.; Cioslowski, J.; Fox, D. J. Gaussian 09, revision D.01; Gaussian, Inc.: Wallingford, CT, 2009. The 3D geometries in the manuscript were generated using CYLview, 1.0b; Legault, C. Y., Université de Sherbrooke, 2009 (http://www. cylview.org).

(42) a) Effect of the damping function in dispersion corrected density functional theory. Grimme, S.; Ehrlich, S.; Goerigk, L. *J. Comput. Chem.* **2011**, *32*, 1456–1465; b) Self-consistent molecular orbital methods. XX. A basis set for correlated wave functions. Krishnan, R.; Binkley, J. S.; Seeger, R.; Pople, J. A. *J. Chem. Phys.* **1980**, *72*, 650–654.

(43) Quantum Mechanical Continuum Solvation Models. Tomasi, J.; Mennucci, B.; Cammi, R. *Chem. Rev.* **2005**, *105*, 2999–3093.

(44) Supramolecular Binding Thermodynamics by Dispersion - Corrected Density Functional Theory. Grimme, S. *Chem. Eur. J.* **2012**, *18*, 9955-9964.

(45) Selected recent examples: a) Chiral Thioureas Promote Enantioselective Pictet–Spengler Cyclization by Stabilizing Every Intermediate and Transition State in the Carboxylic Acid-Catalyzed Reaction. Klausen, R. S.; Kennedy, C. R.; Hyde, A. M.; Jacobsen, E. N. *J. Am. Chem. Soc.* **2017**, *139*, 12299–12309; b) Transition state analysis of an enantioselective Michael addition by a bifunctional thiourea organocatalyst. Izzo, J. A.; Myshchuk, Y.; Hirschi, J. S.; Vetticatt, M. J. *Org. Biomol. Chem.* **2019**, *17*, 3934-3939; c) Isotope Effects Reveal an Alternative Mechanism for "Iminium-Ion" Catalysis. Izzo, J. A.; Poulsen, P. H.; Intrator, J. A.; Jørgensen, K. A.; Vetticatt, M. J. *J. Am. Chem. Soc.* **2018**, *140*, 8396-8400; d) ^{13}C Kinetic Isotope Effects as a Quantitative Probe To Distinguish between Enol and Enamine Mechanisms in Aminocatalysis. Roytman, V. A.; Karugu, R. W.; Hong, Y.; Hirschi, J. S.; Vetticatt, M. J. *Chem. Eur. J.* **2018**, *24*, 8098-8102; e) Catalytic Enantioselective Synthesis of Lactams through Formal [4+2] Cycloaddition of Imines with Homophthalic Anhydride. Jarvis, C. L.; Hirschi, J. S.; Vetticatt, M. J.; Seidel, D. *Angew. Chem. Int. Ed.* **2017**, *56*, 2670-2674.

(46) See the Supporting Information for full computational details.

(47) The lowest energy transition structures with *s*-trans configuration of the ester were 3.4 (*S*) and 3.5 (*R*) kcal/mol higher in energy than the corresponding *s*-cis transition structures. See SI for coordinates.

(48) High-Precision Simultaneous Determination of Multiple Small Kinetic Isotope Effects at Natural Abundance. Singleton, D. A.; Thomas, A. A. *J. Am. Chem. Soc.* **1995**, *117*, 9357–9358.
(49) We also modeled the protonation of the enolate by a protonated piperidine. However, the increased molecularity resulted in a significantly higher free energy barrier.
(50) a) Thiourea Derivatives as Brønsted Acid Organocatalysts. Madarasz, A.; Dosa, Z.; Varga, S.; Soos, T.; Csampai, A.; Papai, I. *ACS Catal.* **2016**, *6*, 4379-4387; b) Stereoselective organocatalyzed glycosylations – thiouracil, thioureas and monothiophthalimide act as Brønsted acid catalysts at low loadings. Bradshaw, G. A.; Colgan, A. C.; Allen, N. P.; Pongener, I.; Boland, M. B.; Ortin, Y. E.; McGarrigle, M. *Chem. Sci*. **2019**, *10*, 508-514.
(51) A comparison can be drawn to the mechanism of Takemoto's *O*-benzylhydroxylamine addition to α,β-unsaturated acids, reactions that are catalyzed by a thiourea catalyst containing both arylboronic acid and tertiary amine functionalities (see reference 14). In these reactions, protonation was also found to be involved in the enantiodetermining step. However, in contrast to the present study where C–N bond formation and protonation represent distinct steps, C–N bond formation is coupled to protonation which occurs in a concerted asynchronous fashion and involves an external carboxylic acid acting as a proton-shuttle. Consistent with the different natures of the two catalytic processes, acidic additives proved detrimental in our case. For instance, addition of catalytic amounts of benzoic acid retarded reaction rates and led to lower enantioselectivities.
(52) ISOEFF98. A program for studies of isotope effects using Hessian modifications. Anisimov, V.; Paneth, P. *J. Math. Chem.* **1999**, *26*, 75-86.
(53) The frequencies were scaled by 0.9614. Harmonic Vibrational Frequencies: An Evaluation of Hartree–Fock, Møller–Plesset, Quadratic Configuration Interaction, Density Functional Theory, and Semiempirical Scale Factors. Scott, A. P.; Radom, L. *J. Phys. Chem.* **1996**, *100*, 16502-16513.g
(54) Bell, R. P. *The Tunnel Effect in Chemistry*; Chapman & Hall: London, 1980.
(55) The final deprotonation of **2a**$_{prot}$ (the intermediate resulting from the catalyst mediated direct C-protonation) to regenerate the catalyst and deliver product (*R*)-**2a** is expected to be facile and is not included in the energy diagram shown in Figure 8.

Table of Contents artwork

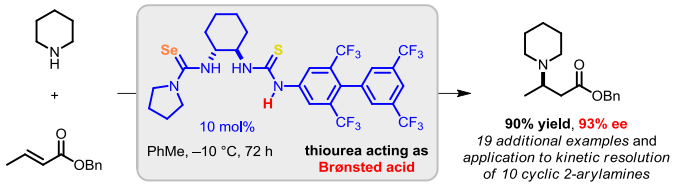

90% yield, **93% ee**
19 additional examples and
application to kinetic resolution
of 10 cyclic 2-arylamines